J Appl Electrochem (2009) 39:253–260
DOI 10.1007/s10800-008-9664-6

ORIGINAL PAPER

Synthesis of functionalized copolymer electrolytes based on polysiloxane and analysis of their conductivity

Fu-Ming Wang · Chi-Chao Wan · Yung-Yun Wang

Received: 30 April 2008 / Accepted: 5 September 2008 / Published online: 25 September 2008

Abstract Functionalized siloxane-based solid polymer electrolytes were synthesized using a platinum-catalyzed silylation reaction. The ionic conductivities of these solid polymer electrolytes were measured as a function of the concentration of lithium bis(trifluoromethylsulfonyl)imide (LiTFSi) salt. The highest ionic conductivity and lowest activation energy of solid polymer electrolytes were observed to be 1.15×10^{-4} S cm^{-1} (25 °C) and 3.85 kJ mol^{-1}, respectively. The interface property between electrolyte and electrode and thermal stability of the polymer electrolytes were found to enhance after they were functionalized with acrylate, and the functionalized electrolytes were observed to maintain a glass transition temperature as low as that of other siloxane compounds. Thus, modifications involving acrylate with ethylene oxide group substitution provide a route for carrier ions and enhance both the ionic conductivity and mechanical properties of the siloxane structure.

F.-M. Wang · C.-C. Wan · Y.-Y. Wang
Department of Chemical Engineering, National Tsing Hua University, 101 Section 2, Kuang Fu Road, Hsinchu 300, Taiwan

C.-C. Wan
e-mail: ccwan@mx.nthu.edu.tw

Y.-Y. Wang
e-mail: yywang@mx.nthu.edu.tw

F.-M. Wang (✉)
Materials and Chemical Research Laboratories, Industrial Technology Research Institute, Rm. 405, Bldg. 77, 195 Sec. 4, Chung Hsing Rd., Chutung, Hsinchu 310, Taiwan
e-mail: mccabe@itri.org.tw

Keywords Solid polymer electrolyte · Polysiloxane · Interface improvement · Ethylene oxide

1 Introduction

The increasing number of accidents involving lithium ion batteries has forced companies such as Apple, IBM, and Nokia to recall large quantities of their products at considerable cost. As a result, manufacturers have been forced to closely consider the safety of these products. Lithium ion batteries containing solid polymer electrolytes have garnered considerable attention since they are much safer, less accident-prone, have high energy storage capacity, and are more reliable [1–5]. In addition, investigations into solid polymer electrolytes (SPE) have demonstrated the feasibility of soft and printable lithium thin film batteries ideal for use in personal electronics. Several of the first generation of solid polymer electrolytes, such as PEO, PAN, and PVDF, have been investigated for their potential as materials in applied electrochemistry [6, 7]. For example, Wright et al. developed a complex of poly(ethylene oxide) (PEO) and alkaline salts, and this was found to exhibit ionic conductivity [8].

In solid polymer electrolytes, lithium ionic transfer is coupled to the local relaxation and segment motion of the PEO chains. This behavior can be observed when PEO is in its amorphous state [9, 10]. However, PEO has poor conductivity ($\sigma \sim 10^{-7}$ S cm^{-1}) due to its high degree of crystallinity at ambient temperatures. To avoid these problems, scientists have developed several approaches, including using metal oxides such as Al_2O_3, TiO_2, and SiO_2, instead of PEO [11–14], as well as atactic poly (propylene oxide) (PPO) randomly copolymerized with

ethylene oxide (EO) [15]. These modifications suppress the vibration of the polymer chains and thereby enhance ionic transfer and prevent crystallization of the matrix polymers [16].

Polysiloxane has a low glass transition temperature (T_g) of −123 °C for poly(dimethylsiloxane), and an extremely high free volume [17] which is often used to mean the excluded volume of a polymer system and the space not taken up by the polymer atoms. This can provide a good ion-hopping site for the transfer of lithium ions to the polymer backbone. In addition, the useful polysiloxane materials also have a hydrosilylative composition consisting of an acrylic, polyester, or epoxy resin with an unsaturated aliphatic bond, a compound having a silylidyne radical, and a hydrosilylation catalyst such as platinum. The hydrosilylation reaction involves subjecting the former two compounds to a hydrosilylation reaction in the presence of the catalyst. Since the hydrosilylation reaction is vigorous, it can be used to cure resin compositions uniformly both at the surface and the interior, with minimal volume loss. Another advantage is that the overall process saves energy, from the initial mixing of components to the end of curing. More recently, Hooper et al. explored use of the hydrosilylation reaction to prepare pendant oligo(ethylene glycol)-substitute chains; the researchers measured the highest conductivity ($\sigma = 4.5 \times 10^{-4}$ S cm^{-1}) at room temperature with lithium bis(trifluoromethylsulfonyl)-imide (LiTFSi) [18]. Furthermore, Lyons et al. have developed oligo(ethylene glycol)methyl ether-substituted side groups and a α,ω-diallyl poly(ethylene glycol) cross-linking reagent have also been developed by [19]. This study measured large ionic conductivities ($\sigma = 1.33 \times 10^{-4}$ S cm^{-1} at the EO:Li ratio of 20:1) at room temperature for polymer networks doped with LiTFSi. However, polysiloxanes are commonly used to form hydrophobic, homogeneous, smooth films on silicon wafers to act as a softening layer and the hydrophobicity polysiloxane prevents the separator, electrode from touching the electrolyte with poor contact ability. This defect will make the interface resistance effect more than ionic conductivity and cannot use in the battery. Besides, the thermal manufacturing treatments have been reported to significantly improve thin film batteries, presumably as a result of electrolyte decomposition and binder phase change.

Therefore, we describe our research to synthesize functionalized poly(methylhydrosiloxane) (PMHS) and poly(ethyl glycol methyl ether methacrylate) (PEGMEMA) using hydrosilylation reactions to avoid the interface problem of polysiloxane electrolyte and also enhance the thermal stability in this research.

2 Experimental

2.1 Materials

Poly(methylhydrosiloxane) (PMHS, $M_w = 1{,}500$–$1{,}900$) and poly(ethyl glycol) methyl ether methacrylate (PEGMEMA, $M_n = 188$, 300, and 475) were purchased from Aldrich. Block copolymer of dimethylsiloxane-(40% ethylene oxide–60% propylene oxide) (DBP-732) with a viscosity of 1,800 Cst. was obtained from Gelest Inc. All of the precursors were dried prior to use for 72 h using a 4 Å molecular sieve. Platinum (0)-1,3-divinyl-1,1,3,3-tetramethyldisiloxane Pt (dvs) was also purchased from Aldrich. A 3 wt% solution of Pt (dvs) in isopropanol was prepared in our laboratory. Lithium bis(trifluoromethylsulfonyl)imide (LiTFSi) was obtained from 3M Co. Nuclear magnetic resonance (NMR)-grade $CDCl_3$ was stored in a glove box.

2.2 The synthesis of functionalized polysiloxane

The hydrosilylation of PMHS was carried out using a platinum catalyst and PEGMEMA. 6.04 g (0.1 mol) of PMHS, 18.38 g (0.1 mol) of $PEGMEMA_{188}$, and 150 mL of tetrahydrofuran (THF) were injected into three 250-mL reaction beakers; 3.04 g (0.1 mol) of PMHS, 16.43 g (0.1 mol) of $PEGMEMA_{300}$, and 150 mL of THF were injected into a 250 mL, three-necked round-bottom flask; and 1.52 g (0.025 mol) of PMHS, 13.06 g (0.025 mol) of $PEGMEMA_{475}$, and 150 mL of THF were injected into three, 250-mL reaction beakers. The molarity ratios of the PEGMEMA and the Si–H group from PMHS were 1:1.05.

The resulting colorless homogeneous solution of mixing solvent with PEGMEMA and THF was heated to 80 °C under N_2. The solution, together with the functionalized polysiloxane precursor and 90 μL of Pt (dvs), was injected into the reactor. This reaction was maintained for 72 h until almost no residual –C=C– or –Si–H groups were detected in the ^{1}H, ^{13}C, or ^{29}Si NMR spectra. The resulting light brown polymer was purified four times with *n*-hexane to remove the catalyst and residual precursors. After purification, the polysiloxane was dissolved in THF and its molecular weight was determined against a polystyrene standard using gel permeation chromatography (GPC).

The molecular weight (M_w) of functionalized polysiloxanes 1, 2, and 3 were 3.8×10^4, 8.9×10^4, and 1.2×10^5 (mol g^{-1}), respectively. The infrared absorbance spectrum indicates a very weak absorption band at 2,160 cm^{-1}, corresponding to ν (Si–H), and a very strong band at 1,104 cm^{-1}, corresponding to ν (Si–O–Si). Polysiloxane 1 exhibits ^{1}H NMR ($CDCl_3$) of δ (ppm) = 4.36 to 4.05, 3.77 to 3.48, 3.39 to 3.37, 1.99 to 1.83, 1.19 to 1.16, 0.93, and 0.15 to 0.12; ^{13}C NMR ($CDCl_3$) of δ (ppm) = 177.2, 77.3 to 76.7,

71.9, 69.2, 68.5, 63.4, 59.0, 45.0 to 44.7, 27.8, and 18.9; and ^{29}Si NMR ($CDCl_3$) of δ (ppm) = −100 to −120 (broad peak). Polysiloxane 2 exhibits ^{1}H NMR ($CDCl_3$) of δ (ppm) = 4.13 to 4.11, 4.08, 3.76 to 3.37, 2.00 to 1.81, 1.31 to 0.86, and 0.20 to 0.11; ^{13}C NMR ($CDCl_3$) of δ (ppm) = 177.6, 77.3 to 76.6, 71.9 to 70.6, 70.5, 68.5, 63.8, 44.8, 29.6 to 29.3, 27.7, 25.6, and 22.2; and ^{29}Si NMR ($CDCl_3$) of δ (ppm) = −100 to −120 (broad peak). Polysiloxane 3 exhibits ^{1}H NMR ($CDCl_3$) of δ (ppm) = 4.07, 3.75 to 3.37, 2.03 to 1.83, 1.31 to 0.86, and 0.06; ^{13}C NMR ($CDCl_3$) of δ (ppm) = 177.4, 77.3 to 76.7, 71.9, 70.6 to 70.5, 68.5, 67.9, 59.0, 45.0, 29.7, and 25.6; and ^{29}Si NMR ($CDCl_3$) of δ (ppm) = −80 to −120 (broad peak).

3 Instrumentation

The solid polymer electrolyte was characterized using a Perkin–Elmer infrared spectrometer (FTIR spectrum 100). The polymer electrolyte was homogeneously deposited on KBr windows. The experiment was repeated at least three times per sample in order to ensure reproducible results. Each scan had a spectral resolution of 2 cm^{-1}; a minimum of 8 scans were averaged to obtain the final result.

Gel permeation chromatography (Alliance GPCV 2000, Waters), using a polystyrene column in the GPC-viscometer module, was used to characterize the molecular weights and weight distributions of the polymers. The flow rate used in the GPC measurements was 1 mL min^{-1} of HPLC-grade THF. Molecular weights were calculated by a standard procedure based on the universal calibration curve of polystyrene.

Calorimetric measurements were performed in a differential scanning calorimeter (Perkin–Elmer DSC-7) under N_2 flow. The DSC temperature controller was calibrated using indium as a standard; the samples were heated from −100 to 300 °C at a heating rate of 10 °C min^{-1}. A liquid nitrogen cooling accessory was used to achieve low temperatures. Glass transition temperatures were defined as the temperatures at the onset of the inflection in the heating curve.

Thermal gram analysis was carried out in a high-resolution thermobalance (TGA-Q500, TA instruments) using a heating rate of 10 °C min^{-1}. Approximately 10 mg of each sample was heated from room temperature to 600 °C under a continuous N_2 flow of 75 mL min^{-1}.

NMR experiments were performed using a Varian UnityINOVA 500 MHz NMR spectrometer equipped with a Chemagnetics 7.5-mm magic angle spinning (MAS) probe and a double-tuned wide-line probe. The ^{1}H and ^{13}C chemical shifts are reported relative to the NMR solvent as an internal standard, and the ^{29}Si chemical shifts are reported relative to an external TMS standard. NMR spectra were recorded using samples dissolved in $CDCl_3$, unless otherwise stated.

Ionic conductivities were measured by AC impedance spectroscopy using a Solatron impedance analyzer (SI-1260) and a potentiostat/galvanostat electrochemical interface (SI-1286) with a frequency range of 0.1–100 kHz, an AC amplitude of 10 mV, and a temperature range of 23–90 °C. The specific ionic conductivity, σ, was obtained from $\sigma = l/AR$, where $l = 0.5$ is the distance between the two stainless steel electrodes, A = 1 cm^2 is the measured area of each electrode, and R is the measured resistance (Ω). The compatibility of the investigated polymer electrolytes with the stainless electrode was determined by AC impedance analysis under open-circuit conditions at different temperatures. The electrolyte contact ability was investigated, and coin cells (2032) were used to measure the resistances of bulk electrolyte and the connectivity between electrolyte and stainless steel electrodes at room temperature.

4 Results and discussion

4.1 Synthesis

Functionalized polysiloxane solid electrolytes were synthesized using the hydrosilylation catalysis method. Precursors with variable –Si–H functionalities were developed by tuning the relative ratios of PMHS and PEGMEMA, as depicted in Scheme 1. The formation of a compound was implied by the light brown color and the absence of reactants in the ^{1}H, ^{13}C, ^{29}Si NMR and FTIR analyses. The proposed mechanism by which the hydrosilylation reaction forms acrylate isomers ($CH_3CH{=}CH_2{-}OR$) involves dissociation of the PMHS ligand and subsequent generation of a solution by the Pt species [18], leading to hydrophilic side outgrowth and coloration of the product. Figure 1 schematically illustrates how the hydrophilic side chain (acrylate isomers) and the hydrophobic main chain (PMHS) of the polysiloxane

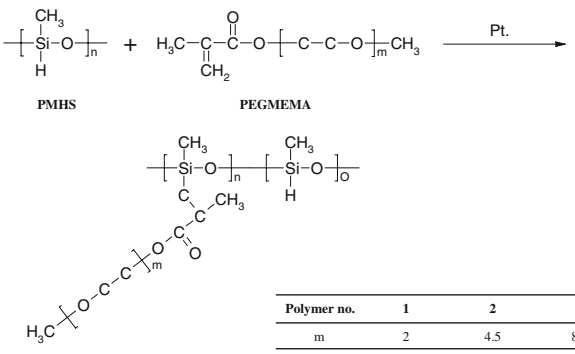

Polymer no.	1	2	3
m	2	4.5	8.5

Scheme 1 Synthesis of hydrophilic polysiloxanes 1–3

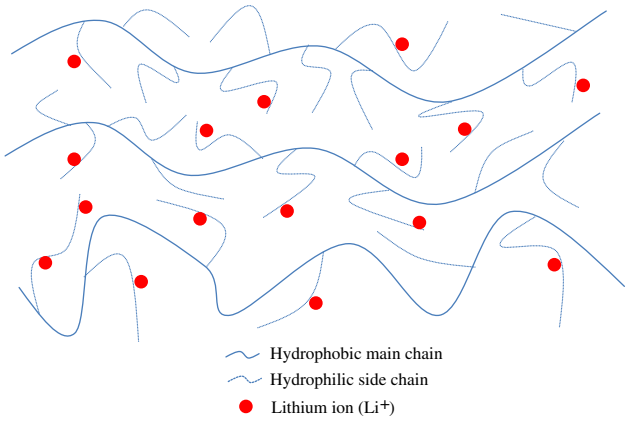

Fig. 1 Schematic illustration of polysiloxane solid state electrolyte

solid electrolyte provide superior routes for lithium ion transfer.

The ^{1}H and ^{29}Si NMR spectra of the precursor and product are depicted in Fig. 2. Figure 2a and b depict a sensitive bonding absorbance difference of 4.7 ppm at the ^{1}H NMR, whereas the reacted functional group of the hydrosilylation reaction does not have an –Si–H group to polysiloxane 3. In addition, the EO side groups appear at 3.25–3.8 ppm as a multilet peak in Fig. 2b, which indicates acrylate synthesis. Moreover, similar evidence appears in the ^{29}Si NMR spectrum, since there is no apparent –Si–H absorbance at −34.7 ppm in contrast to Fig. 3a and b. The ^{1}H NMR spectrum did not reveal any $–CH_2=CH–$ resonance at 5.1 and 5.9 ppm, while FTIR analysis of polysiloxane 3 solid electrolyte after purification confirmed the synthesis of these products: no –Si–H stretch was observed at 2,160 cm^{-1}, and almost no $–CH_2=CH–$ was observed at 1,635 cm^{-1} (Fig. 4). The above data indicate that the reagent reacted to completion.

4.2 Thermal analysis

The thermal properties of the solid polymer electrolytes were characterized by DSC and TGA measurements. The DSC spectra depicted in Fig. 5 provided the glass transition

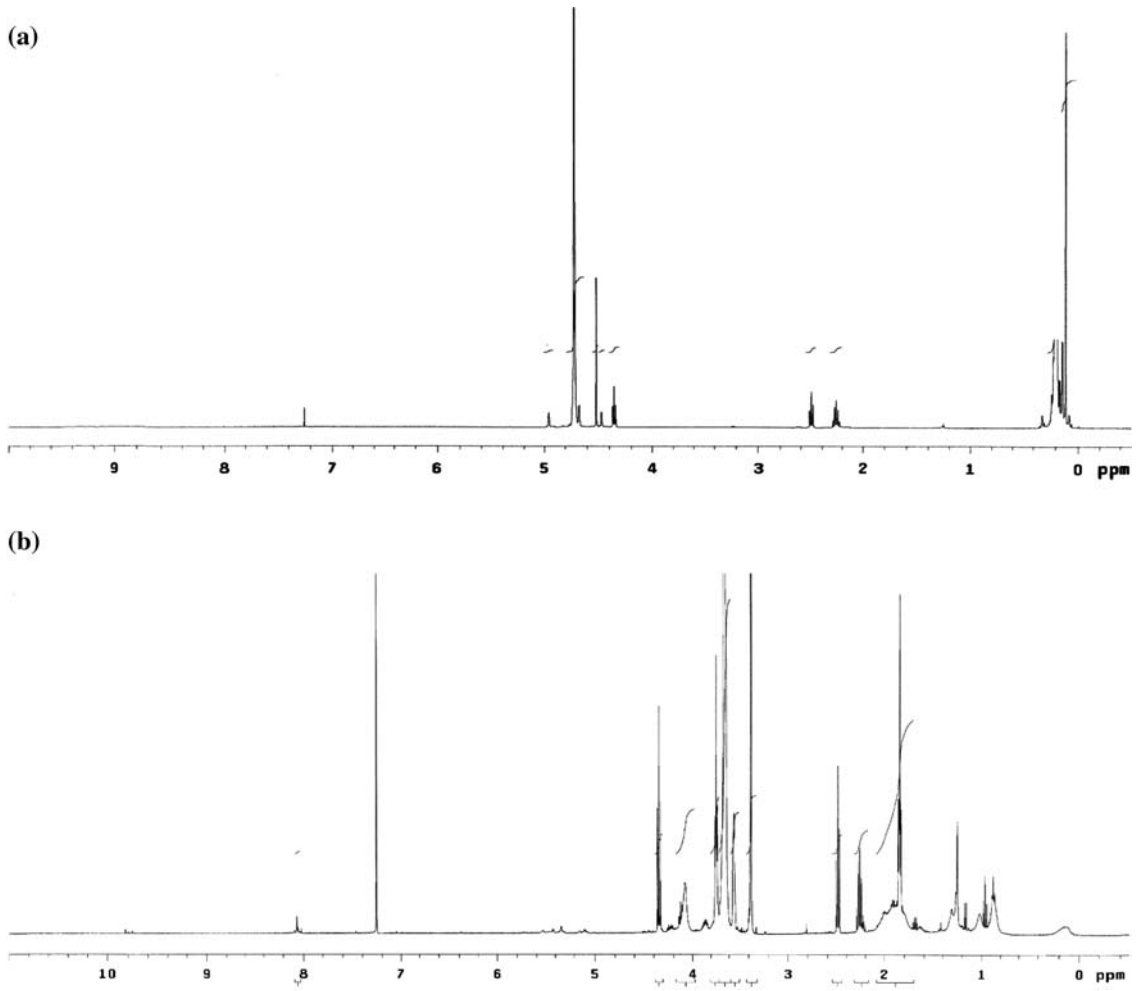

Fig. 2 Representative of ^{1}H NMR spectrum of (**a**) PMHS and (**b**) polysiloxane 3

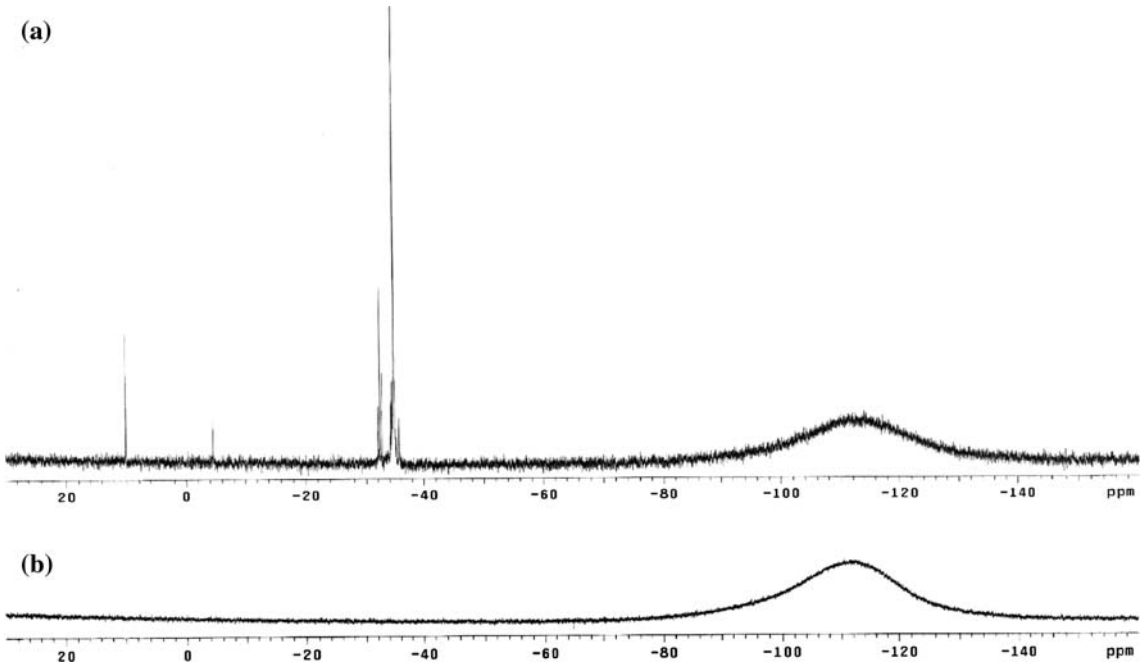

Fig. 3 Representative of ^{29}Si NMR spectrum of (**a**) PMHS and (**b**) polysiloxane 3

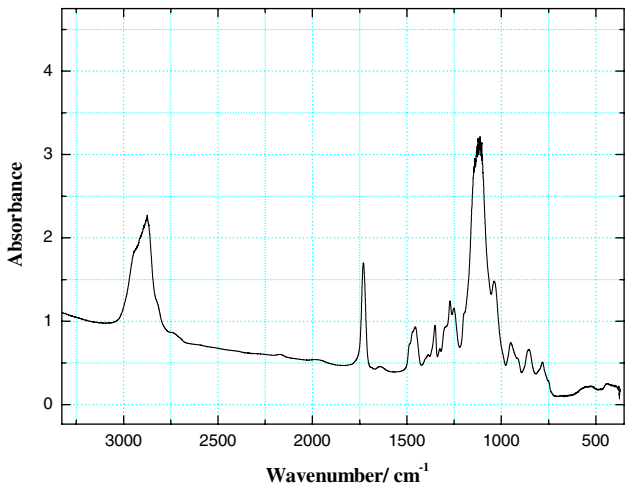

Fig. 4 FTIR absorption spectra of hydrophilic polysiloxane 3

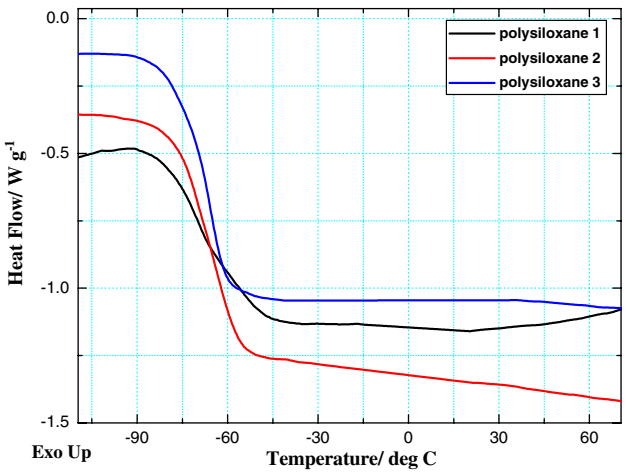

Fig. 5 DSC traces recorded for the hydrophilic polysiloxanes based copolymers

temperatures, T_g, which are listed in Table 1. The glass transition temperatures ranged from −66.3 to −67.9 °C, and the melting temperatures, T_m, ranged from 203.3 to 264.8 °C. As expected, the T_g for polysiloxane was lower than that of poly(ethylene oxide) and was similar to other polysiloxane polymers [17–19]. These values are well below room temperature, and the low values reflect the flexibility of the siloxane segments.

The second set of experiments confirmed the recrystallization of the functionalized polysiloxane, and the T_g of the recrystallized product was the same as that of the original product; hence, a very weak crystallization phenomena and the melting temperature point were observed. These observations indicate that the ethylene oxide-acrylate substituted groups were unable to enhance crystallization.

Table 1 Thermal analysis of hydrophilic polysiloxanes 1–3 without any salt

	DSC, T_g (°C)	DSC, T_m (°C)	DSC, T_d (°C)
Polymer 1	−67.9	203.3	223.5
Polymer 2	−66.3	256.6	282.4
Polymer 3	−67.7	264.8	290.6

The analyses of the thermograms of the polysiloxane polymer are shown in Fig. 6. This figure shows that thermal stability increased with increasing length of the

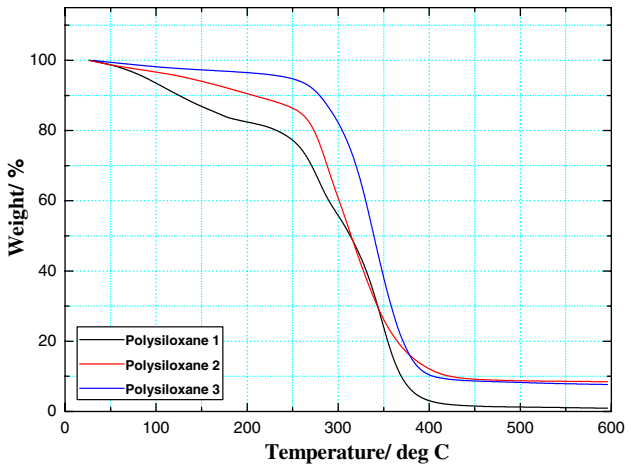

Fig. 6 Thermograms analysis of hydrophilic polysiloxanes-based copolymers

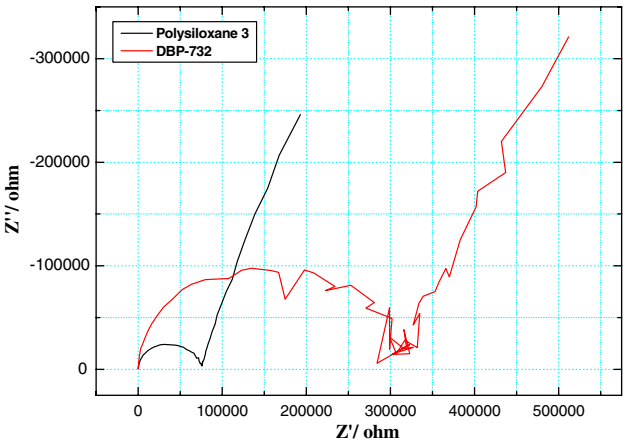

Fig. 7 Electrochemical impedance analysis of hydrophilic polysiloxanes 3 and DBP-732

ethylene oxide-acrylate side chains; this reflects the fact that addition of acrylate enhanced the mechanical properties of the electrolyte. These data suggest that the addition of an optimized ethylene oxide-acrylate side group provides a hopping route for lithium ion transport, and increases the thermal stability of the polymer structure. A 10% reduction in weight was observed for these polymers at temperatures of 125–280 °C. These results suggest that the modified polysiloxane electrolytes are practical for device applications; in other words, the electrolytes are appropriate for use in the high-temperature manufacture of thin film batteries. Furthermore, the decomposition temperature of these functionalized polymer electrolytes was also measured by DSC and were found to be 223–290 °C. The weight loss due to polymer decomposition was confirmed by TGA analysis, which gave the same results as DSC. Because of these properties, use of these novel materials will reduce the cost and complexity of manufacturing.

4.3 Interface property improvement

Several parameters, including ionic conductivity, electrochemical stability, and the interface property of the polymer electrolytes affect the performance of lithium batteries. In addition, in order to improve the connectivity among the electrode, separator, and electrolyte, and also to increase the electrolyte viscidity, Kan et al. [20] developed morphological latex particles using polyacrylate as a viscidating agent, a hydrophilic shell, and polysiloxane as a hydrophobic core. This system showed excellent polymer characteristics. The composition of the electrode consisted of lithium metal oxide and graphite; hence, the hydrophilic compounds can improve the morphology and surface affinity of these electrodes, such as in linear carbonates used for mixing ionic solutions, and in acrylate-based systems for designing polymers [21].

In our polymer electrolyte, the impact of the interface property of the ethylene oxide-acrylate substitute is shown in Fig. 7. We used dimethylsiloxane-(60% propylene oxide/40% ethylene oxide) block copolymer (DBP-732) as the reference polymer. The structure of DBP-732 is similar to normally modified polysiloxanes [17–19, 22, 23], as depicted in Fig. 8. The DBP-732 substituted only ethylene oxide to increase the ionic conductivity. The electrochemistry impedance spectroscopy (EIS) results reveal that the resistance curve of DBP-732 has a substantial semi-circle, which has a larger radius than that of the functionalized polysiloxane electrolyte (polysiloxane 3). The curves also indicate that the electrolytes have the same ionic conductivity with the same initiatory resistances. This suggests that we could only observe the contact variation between reference polymer electrolyte and polysiloxane 3 with the last resistances. The semi-circle displays a conventional equivalent circuit model and can be indentified to a contact resistance from the electrolyte and capacitance from the electron double layer, which is assembled in a parallel model and also contains vibrations in the lower frequency range of 0.1–10 Hz. This suggests that DBP-732 allows poor contact between the electrodes and separator and requires a sine wave with more substantial amplitude to compensate for the resistance at the interface. Furthermore, the Waburg diffusion element was

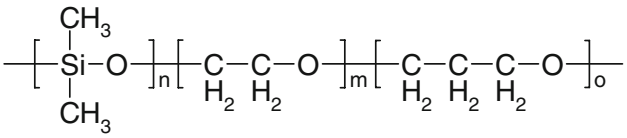

Fig. 8 The structure of dimethylsiloxane-(40% ethylene oxide–60% propylene oxide), DBP-732

connected to the parallel model in series of the two polymer cells.

Even though the electrolytes have good ionic conductivity, the AC impedance indicates that the interface and contact ability to the electrode and separator is sufficient to lower internal resistance and hinder battery performance. DBP-732 still has defects, even though it uses ethylene oxide–propylene oxide as a hopping agent.

4.4 Ionic conductivity

A THF/acetone mixed solvent combined with LiTFSi was used to prepare the functionalized polysiloxane electrolyte and to maximize the dissolution of the salt in the solution. The electrolyte solvent was loaded into a Teflon cell consisting of two stainless steel electrodes, which was then sealed with O-rings. The electrolyte was vacuum-dried at a pressure of less than 1 atm at 35 °C for 48 h to remove the THF/acetone solvent and prevent electrolyte bubbling. The ionic conductivity of the highly viscid, hydrophilic polysiloxane electrolytes were obtained as a function of temperature by AC impedance. Figure 9 depicts the impact of ethylene oxide on the ionic conductivity, and the values of 25, 60 °C are arranged in Table 2.

At temperatures of 25–90 °C, the ionic conductivity increased with increasing EO length at an oxygen: lithium ion molar ratio of 20:1. The impact of EO length on conductivity was reduced as the temperature approached T_g; in other words, the electrolyte had a flexible backbone that effectively supported the hopping mechanism of ion transport. The maximum conductivity of polysiloxane 3 was observed to be $\sigma = 1.15 \times 10^{-4}$ S cm^{-1} at room temperature and 8.04×10^{-4} S cm^{-1} at 60 °C (Table 2).

Arrhenius plots were constructed using the data in Fig. 9. These plots all had the curvature characteristic of

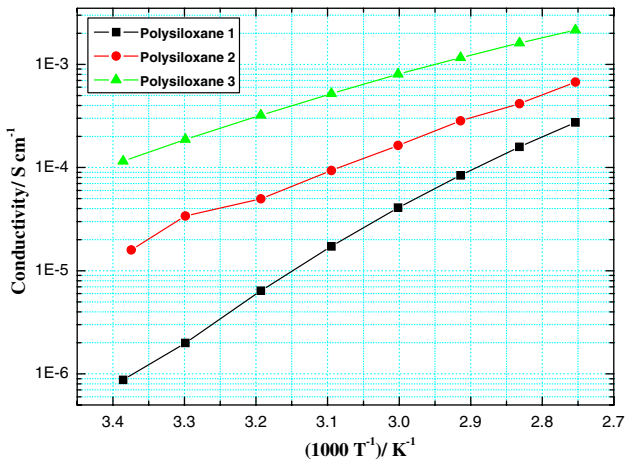

Fig. 9 Ionic conductivity of hydrophilic polysiloxanes 1–3 with various temperature and EO/Li = 20

Table 2 Ionic conducitvity of hydrophilic polysiloxanes 1–3 with EO/Li ratio = 20

	Conductivity, 25 °C (S cm^{-1})	Conductivity, 60 °C (S cm^{-1})
Polymer 1	8.75×10^{-6}	4.05×10^{-5}
Polymer 2	1.59×10^{-5}	1.64×10^{-4}
Polymer 3	1.15×10^{-4}	8.03×10^{-4}

ion transport dependent on the segmental motion of the EO-acrylate chain, as well as the polysiloxane backbone. The Vogel–Tamman–Fulcher (VTF) equation has been used to fit the behavior of the temperature-dependent conductivities of these electrolytes to three values: parameters A, reflecting the number of charge carriers; B, the apparent activation energy; and T_0, the ideal glass transition temperature. The following VTF equation [24] was used to identify the activation energy, E_a, of the Li-ion mobility, with the assumption that the temperature dependence of σ showed VTF behavior. The results are summarized in Table 3.

$$\sigma = AT^{-1/2}e(-B/(T - T_0))$$

These data reveal that polysiloxane 3, which had the greatest number of EO side chains, has the lowest activation energy of 3.85 kJ mol^{-1}. Thus polysiloxane 3 has greater ionic conductivity than the other polysiloxane compounds, indicating that additional EO promotes ionic transfer. In addition, the dependence of the ionic conductivity on increasing EO level can be adequately interpreted as the result of two opposing effects. On the one hand, charge carriers from salt build up as the number of EO side chains increases, but this is eventually offset by a decrease in the flexibility of the polymer structure, which impedes ion migration in the polymer electrolyte with the smallest number of EO side chains.

Figure 10 suggests that the ionic conductivity of polysiloxane 2 depends on the salt concentration. The conductivity values at 25 and 60 °C are shown in Table 4. Interestingly, the crystallinity and melting temperature decreased with increasing Li and EO. Furthermore, the conductivity results of other polysiloxane electrolytes were shown the same. The crystallization rate in the formation of siloxane-based electrolytes may decrease with increasing lithium salt concentration. These data confirm that the solid polymer electrolytes are amorphous over the temperature ranges in

Table 3 Activation energy of hydrophilic polysiloxanes 1–3 with EO/Li ratio = 20

	Polymer 1	Polymer 2	Polymer 3
E_a, activation energy (kJ mol^{-1})	7.67	4.81	3.85

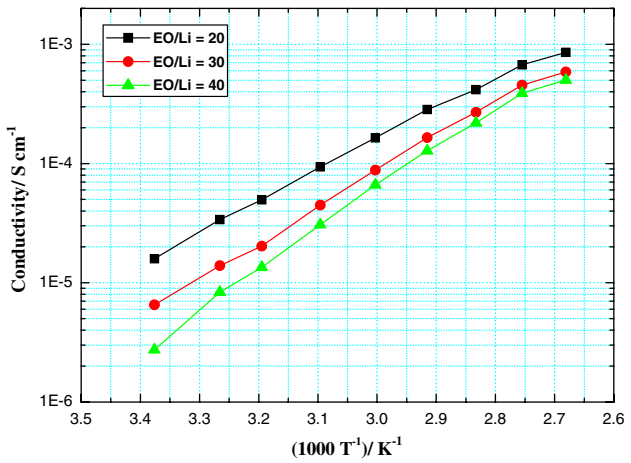

Fig. 10 Ionic conductivity of hydrophilic polysiloxane 2 with various temperature and EO/Li

Table 4 Ionic conductivity of hydrophilic polysiloxanes 2 with EO/Li ratio = 20, 30, 40

EO/Li ratio	Conductivity, 25 °C (S cm^{-1})	Conductivity, 60 °C (S cm^{-1})
20	1.59×10^{-5}	1.64×10^{-4}
30	6.53×10^{-6}	8.83×10^{-5}
40	2.75×10^{-6}	6.63×10^{-5}

Table 5 Activation energy of hydrophilic polysiloxanes 2 with EO/Li ratio = 20, 30, 40

EO/Li ratio	20	30	40
E_a, activation energy (kJ mol^{-1})	4.81	5.57	6.28

which the ionic conductivity measurements were performed. Hence, the maximum ionic conductivities of polysiloxane 2 at room temperature were observed to be 1.59×10^{-5}, 6.53×10^{-6}, and 2.75×10^{-6} S cm^{-1} with EO:Li ratios of 20, 30, and 40, respectively. The same results were observed for the other polysiloxanes, and the results appeared to be independent of temperature. The activation energies are shown in Table 5; they are, respectively, 4.81, 5.57, and 6.28 kJ mol^{-1}. Additional studies on the electrochemical stability, lithium ion transfer, diffusion mechanism, and battery application of these polymer electrolytes are currently being investigated in our laboratory.

5 Conclusion

A series of linear, functionalized viscid polysiloxanes were developed, and they showed excellent ionic conductivity of 1.15×10^{-4} S cm^{-1} at 25 °C in the presence of LiTFSi. Adding acrylate to the polysiloxane electrolyte provided high thermal stability and enhanced the ion transport efficiency as a function of EO content and glass transition temperature. Moreover, this modified polysiloxane electrolyte had an activation energy of 3.85 kJ mol^{-1}, the lowest yet reported in the literature. It also exhibits excellent thermal stability for thin film manufacturing and interface improvement properties, which help it to provide optimal contact with the electrode. Thus these modified polysiloxanes are expected to enhance the operation of thin film lithium batteries.

Acknowledgments Financial support and technical assistance from the Materials and Chemical Research Laboratories at the Industrial Technology Research Institute (Taiwan) are gratefully acknowledged. American Journal Experts is also appreciated for the language assistance.

References

1. Stephon AM (2006) Eur Polym J 42:21
2. Rankin DD, Leal EM, Walther DC (2005) Prog Energy Combust Sci 31:422
3. Allcock HR, Laredo WR, Morford RV (2001) Solid State Ion 139:27
4. Niitani T, Shimada M, Kawamura K, Kanamura K (2005) J Power Sources 146:386
5. Bamford D, Dlubek G, Reiche A, Alam MA, Meyer W, Galvosas P, Rittig F (2001) J Chem Phys 115:7260
6. Gray FM (1991) Solid polymer electrolytes, fundamentals and technological applications. VCH Publishers, New York
7. Gray FM (1997) Polymer electrolytes. The Royal Society of Chemistry Publishers, Cambridge
8. Wright PV (1976) J Polym Sci Polym Phys Ed 14:955
9. Karatas Y, Kaskhedikar N, Burjanadze M, Wiemhofer HD (2006) Macromol Chem Phys 207:419
10. Matsumi N, Nakashiba M, Mizumo T, Ohno H (2005) Macromolecules 38:2040
11. Lin CW, Hung CL, Venkateswarlu M, Hwang BJ (2005) J Power Sources 146:397
12. Hu L, Tang Z, Zhang Z (2007) J Power Sources 166:226
13. Jiang G, Maeda S, Saito Y, Tanase S, Sakai T (2005) J Electrochem Soc 152:A767
14. Croce F (1998) Nature 394:456
15. Watanabe M, Nishimoto A (1995) Solid State Ion 79:306
16. Forsyth M, MacFarlane DR, Best A, Adebahr J, Hill AJ (2002) Solid State Ion 147:203
17. Zhang Z, Sherlock D, West R, West R, Amine K, Lyons JL (2003) Macromolecules 36:9176
18. Hooper R, Lyons LJ, Mapes MK, Schumacher D, Moline DA, West R (2001) Macromolecules 34:931
19. Zhang Z, Lyons LJ, Amine K, West R (2005) Macromolecules 38:5714
20. Kan CY, Kong XZ, Yuan Q, Lin DS (2001) J Appl Polym Sci 80:2251
21. Lin J, Tang Q, Wu J, Hao S (2007) React Funct Polym 67:275
22. Rossi N, Zhang Z, Schneider Y, Morcom K, Lyons L, Wang Q, Amine K, West R (2006) Chem Mater 18:1289
23. Zhang Z, Lyons L, Jin J, Amine K, West R (2005) Chem Mater 17:5646
24. Binesh N, Bhat S (1998) J Polym Sci B 36:1201